Hepatokine ERAP1 impairs skeletal muscle insulin sensitivity via ADRB2/PKA pathway

Feifan Guo (ffguo@sibs.ac.cn)
CAS Key Laboratory of Nutrition, Metabolism and Food Safety, Shanghai Institute of Nutrition and Health, University of Chinese Academy of Sciences, Chinese Academy of Sciences
https://orcid.org/0000-0001-6628-7647

Yuguo Niu
Institute for Nutritional Sciences, Shanghai Institutes for Biological Sciences

Haizhou Jiang
CAS Key Laboratory of Nutrition, Metabolism and Food Safety, Shanghai Institute of Nutrition and Health, University of Chinese Academy of Sciences, Chinese Academy of Sciences
https://orcid.org/0000-0003-4191-221X

Hanrui Yin
CAS Key Laboratory of Nutrition, Metabolism and Food Safety, Shanghai Institute of Nutrition and Health, University of Chinese Academy of Sciences, Chinese Academy of Sciences
https://orcid.org/0000-0003-2373-6339

Fenfen Wang
CAS Key Laboratory of Nutrition, Metabolism and Food Safety, Shanghai Institute of Nutrition and Health, University of Chinese Academy of Sciences, Chinese Academy of Sciences

Xiaoming Hu
CAS Key Laboratory of Nutrition, Metabolism and Food Safety, Shanghai Institute of Nutrition and Health, University of Chinese Academy of Sciences, Chinese Academy of Sciences

Shanghai Chen
Institute for Nutritional Sciences, Shanghai Institutes for Biological Sciences https://orcid.org/0000-0002-0696-2409

Article

Keywords: ADRB2/PKA pathway, Hepatokine ERAP1, skeletal muscle insulin sensitivity

Posted Date: July 7th, 2020

DOI: https://doi.org/10.21203/rs.3.rs-37586/v1

Abstract

The current study aimed to investigate the role of endoplasmic reticulum aminopeptidase 1 (ERAP1), a novel hepatokine, in whole-body glucose metabolism. Here, we found that hepatic ERAP1 levels were increased in insulin-resistant leptin-receptor-mutated (db/db) and high-fat diet (HFD)-fed mice. Consistently, hepatic ERAP1 overexpression attenuated skeletal muscle (SM) insulin sensitivity, whereas knockdown ameliorated SM insulin resistance. Furthermore, serum and hepatic ERAP1 levels were positively correlated, and recombinant mouse ERAP1 or conditioned medium with high ERAP1 content (CM-ERAP1) attenuated insulin signaling in C2C12 myotubes, and CM-ERAP1 or HFD-induced insulin resistance was blocked by ERAP1 neutralizing antibodies. Mechanistically, ERAP1 reduced ADRB2 expression and interrupted ADRB2-dependent signaling in C2C12 myotubes. Finally, ERAP1 inhibition via global knockout or the inhibitor thimerosal improved insulin sensitivity. Together, ERAP1 is a hepatokine that impairs SM and whole-body insulin sensitivity, and its inhibition might provide a therapeutic strategy for diabetes, particularly for those with SM insulin resistance.

Background

The number of type 2 diabetes (T2D) patients is increasing rapidly worldwide, and this is often associated with many metabolic complications, such as hypertension and hyperlipidemia, among others1,2. T2D begins with the development of peripheral insulin resistance, and a previous study has shown that it can commonly originate within the skeletal muscle (SM)3. Because the SM is responsible for more than 80% of insulin-induced glucose uptake and disposal under normal conditions, it is considered the most important organ for whole-body glucose homeostasis, including insulin sensitivity4. Many factors contribute to SM insulin resistance, such as increased serum triglyceride (TG) and free fatty acid (FFA) levels, as well as inflammation, among others5-7. However, insulin sensitivity in SM can also be regulated by secreted proteins from other tissues, such as the liver7-11.

The liver can secrete protein factors called hepatokines to regulate metabolism in other tissues, including the SM7-11. For example, it secretes fibroblast growth factor 2112, fetuin A11, ectodysplasin A8, leukocyte cell-derived chemotaxin 29, and selenoprotein P10 into circulation and regulates insulin sensitivity in the SM. Recent proteomic studies show that the liver might release hundreds to thousands of proteins into circulation13, suggesting that hepatokines are worthy of further investigation.

Endoplasmic aminopeptidase 1 (ERAP1) is a multifunctional enzyme belonging to the M1 family of zinc metallopeptidases14. Its subcellular localization is considered to be inside the endoplasmic reticulum (ER), soluble in the matrix, or anchored to the plasma membrane15. ERAP1 has the potential to trim peptide antigens to optimal lengths for binding to MHC class I molecules in the ER16. Besides, it can bind directly to some inflammatory cytokine receptors, such as type I tumor necrosis factor receptor, and promote their ectodomain shedding to generate soluble receptors and suppress inflammatory response17. ERAP1 also plays a vital role in many autoimmune diseases, such as type I diabetes18, ankylosing spondylitis19, psoriasis20, and Behcet's disease21. Further, it is abundantly expressed in the

liver22 and can also be secreted from hepatocytes as a hepatokine13. The lack of hepatic ERAP1 promotes hepatocellular carcinoma growth in immune-deficient recipients and reduces the efficacy of adoptive T-cell therapy in mice23. However, a function for hepatic and serum ERAP1 in the regulation of whole-body glucose metabolism has not been indicated. Given the fact that another member of the M1 aminopeptidase family, namely placental leucine aminopeptidase, is associated with glucose uptake in adipocytes and SM cells24 and the liver is an important organ that regulates whole-body glucose homeostasis, we hypothesized that hepatic ERAP1 might play an important role in glucose metabolism as a hepatokine.

The aim of our current study was thus to investigate the role of hepatic ERAP1 in the regulation of whole-body glucose metabolism. Our work demonstrates a novel function of hepatic ERAP1 as a hepatokine that regulates SM insulin sensitivity. Moreover, the inhibition of ERAP1 might provide a new therapeutic strategy for diabetes, particularly with respect to SM insulin resistance.

Results

Elevated ERAP1 expression in the liver is related to insulin resistance

Leptin-receptor-mutated (*db/db*) mice are a genetic mouse model with severe insulin resistance25. The liver, as an important organ in the regulation of whole-body glucose homeostasis, exhibits distinct gene expression patterns between *db/db* and C57 BL/6J wild-type (WT) mice26. Interestingly, ERAP1 expression was elevated in the livers of *db/db* mice, but not in white adipose tissue (WAT) or SM, which are also crucial to maintain glucose homeostasis (Figure 1A and Figure S1A). As diet-induced glucose homeostasis dysregulation is more common in the clinic, we further examined ERAP1 expression in mice fed a high-fat diet (HFD) or a control diet for 12 weeks. Similar results were obtained as observed in *db/db* mice (Figure 1B and Figure S1B).

Overexpression of ERAP1 in the liver impairs SM insulin sensitivity in WT mice

To verify the role of liver ERAP1 in regulating physical glucose homeostasis, WT mice were injected with adenovirus expressing ERAP1 (Ad-ERAP1) or control green fluorescent protein (Ad-GFP) via the tail vein. First, we observed that ERAP1 was overexpressed in the livers of mice injected with Ad-ERAP1 (Figure 2A and 2B). Consistent with a role in glucose metabolism regulation, Ad-ERAP1 increased blood glucose and serum insulin levels under both at fed and fasting status, as well as the homeostatic model assessment of insulin resistance (HOMA-IR) index (Figure 2C–2E). By performing glucose tolerance tests (GTTs) and insulin tolerance tests (ITTs), we found that the blood glucose levels decreased much more slowly the

following challenge with glucose or insulin in mice injected with Ad-ERAP1 compared to that in control mice (Figure 2F and 2G).

For further investigation, we conducted an *in vivo* insulin signaling assay by examining the insulin-stimulated phosphorylation of insulin receptor (IR) on Tyr 1150/1151 (p-IR), protein kinase B on Ser473 (p-AKT) and glycogen synthase kinase 3β on Ser 9 (p-GSK3β)27. Consistent with the change in systemic insulin sensitivity, insulin signaling in the SM was significantly impaired, as demonstrated by the decreased levels of p-AKT and p-GSK3β compared to those in control mice (Figure 2H). To our surprise, insulin signaling was not significantly changed in the liver or WAT, though p-IR was slightly increased in the liver of Ad-ERAP1 mice (Figure S2).

Liver-specific knockdown of ERAP1 ameliorates SM insulin resistance

Because the increased level of liver ERAP1 disrupted SM insulin sensitivity, we wondered if decreasing the ERAP1 level in the livers of diabetic mice could improve SM insulin sensitivity. To test this possibility, WT mice injected with negative control adenovirus (Ad-NC) or adenovirus expressing small-hairpin RNA specific for mouse ERAP1 (Ad-shERAP1) were fed a control diet or HFD. ERAP1 protein expression was knocked down in the liver of mice injected with Ad-shERAP1 compared to that in control mice under HFD conditions (Figure 3A). The downregulation of ERAP1 blocked HFD-increased blood glucose and serum insulin levels under both fed and fasting conditions, as well as the HOMA-IR index (Figure 3B-3D). Blood glucose levels decreased much more quickly the following challenge with glucose or insulin in HFD mice injected with Ad-shERAP1 compared to that in control mice as measured by GTTs and ITTs and comparing the differences at each time point, respectively (Figure 3E and 3F).

We also conducted *in vivo* insulin signaling assays and found that SM insulin signaling was significantly enhanced, as demonstrated by the increased protein levels of p-AKT and p-GSK3β (Figure 3G). The changes in insulin signaling in the liver or WAT were not affected or not consistent with whole-body insulin sensitivity, respectively (Figure S3). Similar results were observed in WT mice injected with Ad-shERAP1 under control diet conditions (Figure S4). Moreover, Ad-shERAP1 also improved the parameters above in *db/db* mice (Figure S5).

ERAP1 acts as a hepatokine

We next wondered how altered ERAP1 levels in the liver would affect SM insulin sensitivity. Because ERAP1 can be secreted from the liver as a hepatokine13, we speculated that circulating levels might

regulate SM insulin sensitivity. As predicted, serum ERAP1 levels were elevated in *db/db*, HFD-fed, and Ad-ERAP1 mice, and decreased in mice with the liver-specific knockdown of ERAP1 (Figure 4A–4D). ERAP1 expression in the WAT and SM were not changed in Ad-ERAP1 mice (Figure S6A), suggesting that secreted ERAP1 could not enter the WAT or SM.

To confirm that circulating ERAP1 could regulate SM insulin sensitivity, C2C12 myotubes were incubated with recombinant mouse ERAP1 (rmERAP1), and insulin signaling was impaired, as shown by the decreased levels of p-IR, p-AKT, and p-GSK3β compared to those with control treatment (Figure 4E). rmERAP1 had no influence on insulin signaling in primary hepatocytes or C3H10T1/2 adipocytes (Figure S6B and S6C). The role of secreted ERAP1 was also tested using conditioned medium with a high content of ERAP1 (CM-ERAP1) from HepG2 cells infected with Ad-ERAP1 to treat C2C12 myotubes. We first determined that Ad-ERAP1 increased ERAP1 levels in the CM-ERAP1 (Figure 4F). As expected, CM-ERAP1 impaired insulin signaling in C2C12 myotubes and this effect was reversed by ERAP1 neutralizing antibodies (Figure 4G). Furthermore, we used an ERAP1 neutralizing antibody to block the effect of circulating ERAP1 *in vivo*. Consistently, a single injection of the ERAP1 neutralizing antibodies could improve SM insulin sensitivity in HFD-fed mice, as demonstrated by ITTs and SM insulin signaling, with no effect on the liver and WAT insulin signaling (Figure 4H and 4I, Figure S6D and S6E).

ERAP1 regulates SM insulin sensitivity by decreasing the *β2*-adrenergic receptor (ADRB2) expression

To investigate the cause of SM insulin resistance mediated by serum ERAP1, we performed RNA-seq on the SM of WT mice injected with Ad-GFP or Ad-ERAP1. By conducting KEGG enrichment analysis, we found that the cyclic adenosine monophosphate (cAMP) pathway was enriched remarkably in Ad-ERAP1-injected mice (Figure 5A). As shown previously28, we also observed higher levels of *Adrb2* mRNA in the SM compared to *Adrb1* and *Adrb3* (Figure S7A). In addition, the expression of *Adrb1* or *Adrb3* was not changed in mice with hepatic overexpression of ERAP1 (Figure S7B), suggesting the altered cAMP pathway might be regulated by Adrb2. We then examined some of the genes in this pathway, including *Adrb2*, carnitine palmitoyltransferase 1B, lipoprotein lipase, and catalase29-32. Interestingly, we found that most of them were downregulated, except for *Adrb2*, which was increased (Figure 5B). However, considering that ERAP1 is a proteolytic enzymes33, we speculated that the protein levels of ADRB2 might be downregulated. The protein levels of ADRB2 in the SM of Ad-ERAP1 mice were downregulated as expected, as well as its downstream protein kinase A (PKA) activity34, as demonstrated by phospho-PKA (p-PKA) substrate levels (Figure 5C). Moreover, rmERAP1 also decreased ADRB2 expression and p-PKA substrate levels in C2C12 myotubes (Figure 5D). To further confirm the role of ADRB2 in ERAP1-induced SM insulin resistance, we examined insulin signaling in C2C12 myotubes overexpressing ADRB2 or those stimulated with the adenylyl cyclase activator forskolin35 in the presence of rmERAP1. We found that the overexpression of ADRB2 or treatment with forskolin reversed the suppressive effect of rmERAP1 on

insulin signaling and p-PKA substrate levels in C2C12 myotubes (Figure 5E and 5F). In contrast, treatment with an agonist of the β-adrenergic receptor (β-ARs) isoprenaline36 could not reverse the attenuated insulin signaling and p-PKA substrate levels caused by rmERAP1 in C2C12 myotubes (Figure 5G).

Inhibition of ERAP1 improves insulin sensitivity

Finally, ERAP1-knockout (KO) mice and ERAP1 inhibitors were used to verify the possibility that ERAP1 could be exploited as a drug target for insulin resistance. We generated ERAP1-KO mice and found that ERAP1 levels were almost completely absent in the liver and serum (Figure 6A and 6B). As expected, ERAP1-KO mice exhibited improved glucose metabolism with a decrease in fasting blood glucose levels and the HOMA-IR index, as well as improved GTTs and ITTs, though serum insulin was not changed, as compared to those in WT mice (Figure 6C-6G). We then tested the effect of the ERAP1 inhibitor thimerosal on glucose metabolism in insulin-resistant *db/db* mice. We found that thimerosal significantly ameliorated insulin resistance in these mice, as shown by the corresponding changes in the aforementioned parameters examined (Figure 7A-7E).

Discussion

Different tissues communicate with each other via secreted proteins, metabolites, microRNAs, or other molecules37. Prior studies have shown that proteins secreted from adipocytes (adipokines), such as leptin and adiponectin38,39, as well as those from SM (myokines), including irisin and myostatin40,41, regulate other tissues and whole-body glucose and lipid homeostasis. In addition to adipokines and myokines, hepatokines have gained much attention because some of them were shown to play important roles in many processes8-12, and the liver releases many hepatokines into circulation, with unknown functions that need to be identified13.

Our current study revealed an important function for the hepatokine ERAP1 in regulating insulin sensitivity in the SM and whole-body glucose metabolism. An important effect for hepatic ERAP1 on insulin sensitivity in the SM was shown by the observation that its expression was increased in the livers of insulin-resistant mice; further, the liver-specific overexpression of ERAP1 impaired SM insulin sensitivity and the knockdown of ERAP1 had the opposite effects under basal or insulin-resistant conditions. While investigating the possible mechanisms underlying the hepatic ERAP1 control of insulin sensitivity in the SM, we speculated that some hepatokines might be involved in this regulation. We preferentially considered the involvement of ERAP1 in this regulation because it was previously shown that ERAP1 is a hepatokine13, and serum ERAP1 levels were positively associated with liver ERAP1 levels and increased under conditions of insulin resistance. This possibility was confirmed based on the inhibitory effect of rmERAP1 on insulin signaling in the SM *in vitro*, as well as the ability of neutralizing ERAP1 antibodies to reverse the effect on attenuated insulin signaling in the SM mediated by CM-ERAP1 incubation *in vitro* or HFD-fed mice *in vivo*. Individuals with insulin resistance and prediabetes present

with SM insulin resistance as the earliest abnormality42, and thus, it is crucial to understand the underlying mechanism to prevent the further progression of glucose disorders. Our results provide important insights into the molecular mechanisms underlying SM insulin resistance. Moreover, our results help to understand the mechanisms of crosstalk between the liver and SM that synergistically control whole-body metabolism. Our results also suggest that extensive studies regarding hepatokines need to be carried out.

Though serum ERAP1 levels were increased under conditions of insulin resistance or in mice overexpressing ERAP1, ERAP1 expression was not increased in the SM, suggesting that it is unlikely to function by entering SM cells. As ERAP1 acts as a secreted factor, it is conceivable that it regulates SM insulin sensitivity through a membrane protein. A previous study showed that ERAP1 could promote the shedding of some inflammatory cytokine receptors17. However, it is unlikely that ERAP1 regulates SM insulin sensitivity by targeting inflammatory cytokine receptors, as inflammation typically induces insulin resistance4. We, therefore, tried to identify other membrane proteins by conducting RNA-seq analysis of SM in Ad-ERAP1-injected WT mice and performing KEGG pathway analysis. In mice injected with Ad-ERAP1, we noticed that many of the differentially expressed genes were enriched in the cAMP signaling pathway, which is under control of β-ARs43. β-ARs are G protein-coupled receptors expressed in most tissues44. Norepinephrine binds to, and actives β-ARs and subsequently activates protein kinase A (PKA)34, which has been shown to play an important role in regulating lipid and glucose metabolism45,46. There are three subtypes of β-ARs (β1, β2, and β3) and the SM of mice preferentially expresses β2AR28. Consistent with the results of a previous report28, we also observed higher levels of *Adrb2* mRNA in the SM. Even though different tissues act distinctly on the stimulation of β2AR, glucose metabolism in the SM was improved in almost all prior studies28,47. In our work, we showed that ERAP1 causes SM insulin resistance by reducing β2AR expression as demonstrated by the fact that β2AR levels were reduced by rmERAP1; further, the overexpression of β2AR or stimulation of a β2AR downstream effector reversed the attenuated insulin signaling and β2AR levels inhibited by rmERAP1 in C2C12 myotubes. However, an *in vivo* study will be required to confirm this mechanism. Furthermore, the molecular mechanisms underlying the ERAP1 regulation of β2AR expression is unclear. As ERAP1 is a proteolytic enzyme that promotes the ectodomain shedding of some inflammatory cytokine receptors17, we hypothesized that it might similarly reduce β2AR expression. This possibility needs to be studied in the future.

The liver-specific knockdown of ERAP1 improves SM insulin sensitivity in mice under normal or insulin-resistant conditions, suggesting that ERAP1 might be a potential drug target to treat SM insulin resistance. To further explore this possibility, we inhibited ERAP1 activity through the global knockout of ERAP1 in mice. Consistent with a previous report48, we observed that ERAP1-KO mice appear normal. However, they exhibited improved insulin sensitivity. Furthermore, our work shows that the inhibition of ERAP1 via its inhibitors or a neutralizing antibody reverses SM and whole-body insulin resistance in *db/db* mice or HFD-fed mice. These results suggest that hepatic and serum ERAP1 might be a potential drug target to treat insulin resistance in the SM.

However, there are still several questions. We noticed that the phosphorylation of IR was not affected by Ad-ERAP1 *in vivo*, but it was significantly inhibited by rmERAP1 or CM-ERAP1 in the SM *in vitro.* We speculate that there are some other factors in the serum from other tissues that can also regulate the phosphorylation of IR. This possibility requires further study. Another question is that the distinct role of serum ERAP1 in regulating insulin signaling in different tissues, as we found that ERAP1 only attenuated insulin signaling in the SM but had no significant effect on insulin signaling in the WAT or liver. This is possibly due to the preferential expression of different isoforms of βARs in different tissues49. ERAP1 has significant effects on β2AR expression, which is the dominant isoform expressed in the SM; however, the WAT mainly expresses β3AR, and the liver expresses mainly β1AR and β2AR49. Therefore, ERAP1 might have different effects on insulin signaling in different tissues. However, these possibilities need to be studied in the future.

The reasons for the upregulated expression of hepatic ERAP1 in insulin-resistant mice also remain unknown. Recent work reported that interferon γ (IFN-γ) induces interferon regulatory factor 1 expression, which is a transcription factor that increases the expression of ERAP150. Considering that *db/db* mice and HFD-fed mice have increased levels of IFN-γ in the liver 51, we speculate that this pathway might be involved in the regulation of ERAP1 in the livers of insulin-resistant mice. Future work will be required to explore this possibility.

Taken together, our work demonstrated that hepatic, along with serum ERAP1 levels were elevated in *db/db* or HFD-fed mice. Increased serum ERAP1 interrupted with ADRB2/PKA signaling and caused SM insulin resistance (Figure 7F). The inhibition of ERAP1 by a neutralizing antibody or inhibitors could improve whole-body glucose hemostasis, and especially SM insulin sensitivity. These results provide valuable insights into the molecular mechanisms underlying SM insulin resistance, especially in a tissue crosstalk manner. Our results also suggest a potential drug target to target insulin resistance, and particularly SM insulin resistance. Because SM insulin resistance is an early sign of whole-body insulin resistance3, increased ERAP1 might also be a possible biomarker to detect the early stage of insulin resistance, which will be important to prevent the progression of diabetes.

Methods

Animals

Male C57BL/6J WT mice were obtained from Shanghai Laboratory Animal Co., Ltd. (Shanghai, China). Leptin receptor-mutated (*db/db*) mice were obtained from the Model Animal Research Center of Nanjing University (Nanjing, China). ERAP1 hybrid knockout (*Erap1+/−*) mice were generated using CRISPR/Cas9 technology, and the guide RNAs (gRNAs) were targeted at the intron 2 and intron 3 of *Erap1* (Shanghai Model Organisms Center, Shanghai, China).

Erap1+/− mice were back-crossed to WT mice for at least two generations to generate Erap1 global KO mice. For all experiments, littermates of the same sex (male) were randomly assigned to experimental

groups. For the HFD feeding experiment, 4-week-old WT mice were fed either a control diet or 60% HFD (Research Diets, NJ, USA) for 4 months. For ERAP1 inhibitor, thimerosal52 experiments, mice were intraperitoneally (i.p.) injected with thimerosal (Sigma, MO, USA) at a dose of 6 mg/kg53 or PBS for 6 days. For neutralizing antibody injection, mice were singly i.p. injected with anti-ERAP1 neutralizing antibodies or control IgG (R&D system, USA) at a dose of 1 mg/kg 30 min before experiments. Mice were maintained with a 12-h light/dark cycle at 23 °C. All anim al experiments were performed in accordance with the guidelines of the Institutional Animal Care and Use Committee of Shanghai Institute of Nutrition and Health, Chinese Academy of Sciences (CAS).

Cell culture and treatments

HEK 293 (ATCC, CRL-1573), Hep G2 (ATCC, HB-8065), C3H/10T1/2 (ATCC, CCL-226), and C2C12 (ATCC, CRL-1772) cell lines were purchased from Cell Bank of Shanghai Institute of Cell Biology, CAS. Mouse primary hepatocytes were prepared by collagenase perfusion as described previously54. Cells were cultured in DMEM (Invitrogen, Carlsbad, CA, USA) with 10% fetal bovine serum, 100 units/ml penicillin, and 100 μg/ml streptomycin sulfate. The differentiation of C2C12 myoblasts55 and C3H/10T1/2 preadipocytes56 was induced, as previously described. C2C12 myotubes, C3H/10T1/2 adipocytes, or primary hepatocytes were incubated with CM-ERAP157 or rmERAP1 (R&D system, USA)58 at the indicated concentration for the indicated time. To detect insulin signaling, C2C12 myotubes, primary hepatocytes, and C3H/10T1/2 adipocytes were incubated with 100 nM insulin for 20 min27,55,59.

Recombinant adenoviruses

The DNA fragments encoding ERAP1 and ADRB2 were amplified from mouse liver cDNA. The recombinant adenovirus expressing mouse ERAP1 (Ad-ERAP1) or ADRB2 (Ad-ADRB2) was generated using the AdEasy™ Adenoviral Vector System (Qbiogene, Irvine, CA, USA) and Ad-NC or Ad-shERAP1 was generated using the BLOCK-iT™ Adenoviral RNAi Expression System (Invitrogen, Carlsbad, CA, USA), according to the manufacturer's instructions. The shRNA sequence for mouse ERAP1 was 5'-CCAGCACCATTATTATGCATAGTCA-3'. Purified high-titer stocks of amplified recombinant adenoviruses were diluted in PBS and injected via the tail vein at a dose of 1 ´ 109 pfu /mice for a single injection54.

High-ERAP1 conditioned medium

HepG2 cells were infected with Ad-GFP or Ad-ERAP1 at a dose of 107 pfu/well in 12-well plates and changed with fresh medium 24 h later54; CM-ERAP1 was collected at 48 and 72 h, as described previously60.

Insulin resistance associated parameters

Blood glucose was measured with a Glucometer Elite monitor (Optium Xceed, IL, USA). Serum insulin was determined based on an ELISA using the Mercodia Ultrasensitive Rat Insulin ELISA kit (ALPCO Diagnostic, NH, USA) in accordance with the manufacturer's instructions. After 14 h of overnight fasting, GTTs were conducted via the i.p. injection of 2 g/kg glucose. For ITTs, mice were injected with 0.75 or 1 U/kg insulin after 4 h of fasting. The HOMA-IR index was calculated as follows: [fasting glucose levels (mmol/l)] ´ [fasting serum insulin (μU/ml)] / 22.554.

In vivo insulin signaling assay

Mice were fasted for 6 h prior to insulin injection, as previously described27. Small sections of the soleus muscle, WAT, and liver were excised from anesthetized live mice and kept as untreated controls. Insulin was injected at a dose of 2 U/kg into WT mice or at 5 U/kg in *db/db* mice via the portal vein; a small piece of the liver section was excised for western blot analysis after 3 min. Another side WAT and soleus muscle were excised after 4 and 5 min.

Western blot analysis

Western blot analysis was performed as previously described27. Primary antibodies obtained are as follows: anti-p-IR (tyr1150/1151), anti-IR, anti-p-AKT (ser473), anti-AKT, anti-p-GSK3β (ser 9), anti-GSK3β, and anti-p-PKA substrates (Cell Signaling Technology, Beverly, MA, USA); anti-ERAP1 (Abcam, Cambridge, England); anti-ADRB2 and anti-β-actin (Protein Tech, Chicago, USA); anti-α-tubulin and anti-ADRB1 (Sigma-Aldrich, St. Louis, USA); anti-ADRB3 (Signalway Antibody, Maryland, USA). All of these assays were performed according to the manufacturer's instructions.

Relative RT-PCR and Illumina deep sequencing

Total RNA was extracted from mouse tissue samples using TRIzol reagent (Invitrogen, Waltham, MA, USA) as previously described54. mRNA levels were examined by RT-PCR with thebprimers described in Table S1. The samples were also sequenced using the Illumina HiSeq™ 4000 system at Shanghai Majorbio Bio-pharm Biotechnology Co., Ltd. (Shanghai, China). The data were analyzed with the free online platform Majorbio Cloud Platform (www.majorbio.com)

Quantification and statistical analysis

Statistical analysis was performed using GraphPad Prism, version 8.0 (GraphPad Software, San Diego, CA). All data are expressed as the mean ± SEM. Significant differences were assessed either by an unpaired two-tailed student *t-test* or one-way ANOVA followed by the Student-Newman-Keuls (SNK) test, as indicated. For GTTs and ITTs, a *t-test* or one-way ANOVA was used to compare the difference between groups at each time points examined. $P < 0.05$ was considered statistically significant.

References

1. Pinhas-Hamiel, O. & Zeitler, Acute and chronic complications of type 2 diabetes mellitus in children and adolescents. *Lancet* **369**, 1823-1831, doi:10.1016/S0140-6736(07)60821-6 (2007).
2. Chatterjee, S., Khunti, K. & Davies, M. J. Type 2 diabetes. *Lancet* **389**, 2239-2251, doi:10.1016/S0140-6736(17)30058-2 (2017).
3. Greene, N. *et al.* Skeletal Muscle Insulin Resistance as a Precursor to Diabetes: Beyond Glucoregulation. *Current diabetes reviews* **14**, 113-128, doi:10.2174/1573399813666161122123636 (2018).
4. Wu, & Ballantyne, C. M. Skeletal muscle inflammation and insulin resistance in obesity. *J Clin Invest* **127**, 43-54, doi:10.1172/jci88880 (2017).
5. Abdul-Ghani, M. A. & DeFronzo, R. A. Pathogenesis of insulin resistance in skeletal muscle. *J Biomed Biotechnol* **2010**, 476279, doi:10.1155/2010/476279 (2010).
6. Di Meo, , Iossa, S. & Venditti, P. Skeletal muscle insulin resistance: role of mitochondria andother ROS sources. *J Endocrinol* **233**, R15-r42, doi:10.1530/joe-16-0598 (2017).
7. Khan, I. M. *et al.* Intermuscular and perimuscular fat expansion in obesity correlates with skeletal muscle T cell and macrophage infiltration and insulin resistance. *International journal of obesity (2005)* **39**, 1607-1618, doi:10.1038/ijo.2015.104 (2015).
8. Awazawa, *et al.* A microRNA screen reveals that elevated hepatic ectodysplasin A expression contributes to obesity-induced insulin resistance in skeletal muscle. *Nat Med* **23**, 1466-1473, doi:10.1038/nm.4420 (2017).

9. Lan, *et al.* LECT2 functions as a hepatokine that links obesity to skeletal muscle insulin resistance. *Diabetes* **63**, 1649-1664, doi:10.2337/db13-0728 (2014).
10. Misu, H. *et al.* A liver-derived secretory protein, selenoprotein P, causes insulin resistance. *Cell Metab* **12**, 483-495, doi:10.1016/j.cmet.2010.09.015 (2010).
11. Pal, D. *et al.* Fetuin-A acts as an endogenous ligand of TLR4 to promote lipid-induced insulin resistance. *Nat Med* **18**, 1279-1285, doi:10.1038/nm.2851 (2012).
12. Kharitonenkov, A. *et al.* FGF-21 as a novel metabolic regulator. *J Clin Invest* **115**, 1627-1635, doi:10.1172/jci23606 (2005).
13. Meex, R. C. *et al.* Fetuin B Is a Secreted Hepatocyte Factor Linking Steatosis to Impaired Glucose Metabolism. *Cell Metab* **22**, 1078-1089, doi:10.1016/j.cmet.2015.09.023 (2015).
14. Cifaldi, L., Romania, , Lorenzi, S., Locatelli, F. & Fruci, D. Role of endoplasmic reticulum aminopeptidases in health and disease: from infection to cancer. *Int J Mol Sci* **13**, 8338-8352, doi:10.3390/ijms13078338 (2012).
15. Peer, A. The role of multifunctional M1 metallopeptidases in cell cycle progression. *Ann Bot***107**, 1171-1181, doi:10.1093/aob/mcq265 (2011).
16. Serwold, , Gonzalez, F., Kim, J., Jacob, R. & Shastri, N. ERAAP customizes peptides for MHC class I molecules in the endoplasmic reticulum. *Nature* **419**, 480-483, doi:10.1038/nature01074 (2002).
17. Cui, X. *et al.* Identification of ARTS-1 as a novel TNFR1-binding protein that promotes TNFR1 ectodomain shedding. *J Clin Invest* **110**, 515-526, doi:10.1172/JCI13847 (2002).
18. Thomaidou, S. *et al.* β-Cell Stress Shapes CTL Immune Recognition of Preproinsulin Signal Peptide by Posttranscriptional Regulation of Endoplasmic Reticulum Aminopeptidase 1. *Diabetes* **69**, 670-680, doi:10.2337/db19-0984 (2020).
19. Burton, R. *et al.* Association scan of 14,500 nonsynonymous SNPs in four diseases identifiesautoimmunity variants. *Nature genetics* **39**, 1329-1337, doi:10.1038/ng.2007.17 (2007).
20. Wiśniewski, A. *et al.* The association of ERAP1 and ERAP2 single nucleotide polymorphisms and their haplotypes with psoriasis vulgaris is dependent on the presence or absence of the HLA-C*06:02 allele and age at disease onset. *Human immunology* **79**, 109-116, doi:10.1016/j.humimm.2017.11.010 (2018).
21. Fierabracci, A., Milillo, A., Locatelli, & Fruci, D. The putative role of endoplasmic reticulum aminopeptidases in autoimmunity: insights from genomic-wide association studies. *Autoimmun Rev* **12**, 281-288, doi:10.1016/j.autrev.2012.04.007 (2012).
22. Miyashita, H. *et al.* A mouse orthologue of puromycin-insensitive leucyl-specific aminopeptidase is expressed in endothelial cells and plays an important role in angiogenesis. *Blood* **99**, 3241-3249, doi:10.1182/blood.v99.9.3241 (2002).
23. Schmidt, K. *et al.* ERAP1-Dependent Antigen Cross-Presentation Determines Efficacy of Adoptive T-cell Therapy in *Cancer research* **78**, 3243-3254, doi:10.1158/0008-5472.can-17-1946 (2018).

24. Keller, S. R. The insulin-regulated aminopeptidase: a companion and regulator of *Frontiers in bioscience : a journal and virtual library* **8**, s410-420, doi:10.2741/1078 (2003).
25. Gomez-Banoy, N. *et al.* Adipsin preserves beta cells in diabetic mice and associates with protection from type 2 diabetes in humans. *Nat Med* **25**, 1739-1747, doi:10.1038/s41591-019-0610-4 (2019).
26. Zhang, *et al.* Gene expression profile analysis of type 2 diabetic mouse liver. *PloS one* **8**, e57766, doi:10.1371/journal.pone.0057766 (2013).
27. Yu, *et al.* PRLR regulates hepatic insulin sensitivity in mice via STAT5. *Diabetes* **62**, 3103-3113, doi:10.2337/db13-0182 (2013).
28. Shiuchi, *et al.* Hypothalamic orexin stimulates feeding-associated glucose utilization in skeletal muscle via sympathetic nervous system. *Cell Metab* **10**, 466-480, doi:10.1016/j.cmet.2009.09.013 (2009).
29. Castejón -Griñán, , Herraiz, C., Olivares, C., Jiménez -Cervantes, C. & García -Borrón, J. C. cAMP-independent non-pigmentary actions of variant melanocortin 1 receptor: AKT-mediated activation of protective responses to oxidative DNA damage. *Oncogene* **37**, 3631-3646,doi:10.1038/s41388-018-0216-1 (2018).
30. Kok, B. , Dyck, J. R., Harris, T. E. & Brindley, D. N. Differential regulation of the expressions of the PGC-1α splice variants, lipins, and PPARα in heart compared to liver. *Journal of lipid research* **54**, 1662-1677, doi:10.1194/jlr.M036624 (2013).
31. Lian, A., Wu, , Liu, T., Jiang, N. & Jiang, Q. Adropin induction of lipoprotein lipase expression in tilapia hepatocytes. *Journal of molecular endocrinology* **56**, 11-22, doi:10.1530/jme-15-0207 (2016).
32. Nikolaev, O. *et al.* Beta2-adrenergic receptor redistribution in heart failure changes cAMP compartmentation. *Science (New York, N.Y.)* **327**, 1653-1657, doi:10.1126/science.1185988 (2010).
33. Hattori, A., Matsumoto, H., Mizutani, S. & Tsujimoto, M. Molecular cloning of adipocyte-derived leucine aminopeptidase highly related to placental leucine aminopeptidase/oxytocinase. *J Biochem* **125**, 931-938, doi:10.1093/oxfordjournals.jbchem.a022371 (1999).
34. Sun, Z. *et al.* Norepinephrine inhibits the cytotoxicity of NK92MI cells via the beta2adrenoceptor/cAMP/PKA/pCREB signaling pathway. *Molecular medicine reports* **17**, 8530-8535, doi:10.3892/mmr.2018.8872 (2018).
35. Sapio, L. *et al.* The Natural cAMP Elevating Compound Forskolin in Cancer Therapy: Is It Time? *Journal of cellular physiology* **232**, 922-927, doi:10.1002/jcp.25650 (2017).
36. Scotney, *et al.* Glucocorticoids modulate human brown adipose tissue thermogenesis in vivo.*Metabolism: clinical and experimental* **70**, 125-132, doi:10.1016/j.metabol.2017.01.024 (2017).
37. Choi, C. H. J. & Cohen, Adipose crosstalk with other cell types in health and disease.*Experimental cell research* **360**, 6-11, doi:10.1016/j.yexcr.2017.04.022 (2017).
38. Perry, R. J. *et al.* Leptin Mediates a Glucose-Fatty Acid Cycle to Maintain Glucose Homeostasis in Starvation. *Cell* **172**, 234-248.e217, doi:10.1016/j.cell.2017.12.001 (2018).

39. Yanai, & Yoshida, H. Beneficial Effects of Adiponectin on Glucose and Lipid Metabolism and Atherosclerotic Progression: Mechanisms and Perspectives. *Int J Mol Sci* **20**, doi:10.3390/ijms20051190 (2019).
40. Boström, *et al.* A PGC1-α-dependent myokine that drives brown-fat-like development of white fat and thermogenesis. *Nature* **481**, 463-468, doi:10.1038/nature10777 (2012).
41. Rao, R. R. *et al.* Meteorin-like is a hormone that regulates immune-adipose interactions to increase beige fat thermogenesis. *Cell* **157**, 1279-1291, doi:10.1016/j.cell.2014.03.065 (2014).
42. Abdul-Ghani, M. A., Jenkinson, C. , Richardson, D. K., Tripathy, D. & DeFronzo, R. A. Insulinsecretion and action in subjects with impaired fasting glucose and impaired glucose tolerance: resultsfrom the Veterans Administration Genetic Epidemiology Study. *Diabetes* **55**, 1430-1435, doi:10.2337/db05-1200 (2006).
43. Berthouze, M., Laurent, A. C., Breckler, M. & Lezoualc'h, New perspectives in cAMP-signaling modulation. *Current heart failure reports* **8**, 159-167, doi:10.1007/s11897-011-0062-8 (2011).
44. Xie, L. *et al.* Oxygen-regulated beta(2)-adrenergic receptor hydroxylation by EGLN3 and ubiquitylation by pVHL. *Science signaling* **2**, ra33, doi:10.1126/scisignal.2000444 (2009).
45. Deng, J. *et al.* Deletion of ATF4 in AgRP Neurons Promotes Fat Loss Mainly via Increasing Energy Expenditure. *Diabetes* **66**, 640-650, doi:10.2337/db16-0954 (2017).
46. Gastaldi, G. *et al.* Upregulation of peroxisome proliferator-activated receptor gamma coactivator gene (PGC1A) during weight loss is related to insulin sensitivity but not to energy expenditure. *Diabetologia* **50**, 2348-2355, doi:10.1007/s00125-007-0782-1 (2007).
47. Kato, E., Inagaki, & Kawabata, J. Higenamine 4'-O-β-d-glucoside in the lotus plumule induces glucose uptake of L6 cells through β2-adrenergic receptor. *Bioorganic & medicinal chemistry* **23**, 3317-3321, doi:10.1016/j.bmc.2015.04.054 (2015).
48. Firat, E. *et al.* The role of endoplasmic reticulum-associated aminopeptidase 1 in immunity to infection and in cross-presentation. *J Immunol* **178**, 2241-2248, doi:10.4049/jimmunol.178.4.2241 (2007).
49. Shi, *et al.* β2-Adrenergic receptor ablation modulates hepatic lipid accumulation and glucose tolerance in aging mice. *Experimental gerontology* **78**, 32-38, doi:10.1016/j.exger.2016.03.005 (2016).
50. Kriegsman, B. A. *et al.* Frequent Loss of IRF2 in Cancers Leads to Immune Evasion through Decreased MHC Class I Antigen Presentation and Increased PD-L1 Expression. *J Immunol* **203**, 1999-2010, doi:10.4049/jimmunol.1900475 (2019).
51. Zhou, D. *et al.* Total fecal microbiota transplantation alleviates high-fat diet-induced steatohepatitis in mice via beneficial regulation of gut microbiota. *Sci Rep* **7**, 1529, doi:10.1038/s41598-017-01751-y (2017).
52. Stamogiannos, A., Papakyriakou, A., Mauvais, X., van Endert, P. & Stratikos, E. Screening Identifies Thimerosal as a Selective Inhibitor of Endoplasmic Reticulum Aminopeptidase 1. *ACS Med Chem Lett* **7**, 681-685, doi:10.1021/acsmedchemlett.6b00084 (2016).

53. Olczak, , Duszczyk, M., Mierzejewski, P. & Majewska, M. D. Neonatal administration of a vaccine preservative, thimerosal, produces lasting impairment of nociception and apparent activation of opioid system in rats. *Brain research* **1301**, 143-151, doi:10.1016/j.brainres.2009.09.003 (2009).
54. Guo, *et al.* A Novel Function of Hepatic FOG2 in Insulin Sensitivity and Lipid Metabolism Through PPARalpha. *Diabetes* **65**, 2151-2163, doi:10.2337/db15-1565 (2016).
55. Sun, C. *et al.* SIRT1 improves insulin sensitivity under insulin-resistant conditions by repressing PTP1B. *Cell Metab* **6**, 307-319, doi:10.1016/j.cmet.2007.08.014 (2007).
56. Li, S. *et al.* Downregulation of β1,4-galactosyltransferase 5 improves insulin resistance by promoting adipocyte commitment and reducing inflammation. *Cell death & disease* **9**, 196, doi:10.1038/s41419-017-0239-5 (2018).
57. Chen, C. , Chen, Y. Y., Huang, J. P. & Wu, Y. H. The effect of conditioned medium derived from human placental multipotent mesenchymal stromal cells on neutrophils: possible implications for placental infection. *Mol Hum Reprod* **20**, 1117-1125, doi:10.1093/molehr/gau062 (2014).
58. Goto, , Ogawa, K., Hattori, A. & Tsujimoto, M. Secretion of endoplasmic reticulum aminopeptidase 1 is involved in the activation of macrophages induced by lipopolysaccharide and interferon-gamma. *J Biol Chem* **286**, 21906-21914, doi:10.1074/jbc.M111.239111 (2011).
59. Burgermeister, E. *et al.* A novel partial agonist of peroxisome proliferator-activated receptor-gamma (PPARgamma) recruits PPARgamma-coactivator-1alpha, prevents triglyceride accumulation, and potentiates insulin signaling in vitro. *Molecular endocrinology (Baltimore, Md.)* **20**, 809-830, doi:10.1210/me.2005-0171 (2006).
60. Horvat, S., Mahnic, A., Breskvar, M., Dzeroski, S. & Rupnik, M. Evaluating the effect of Clostridium difficile conditioned medium on fecal microbiota community structure. *Sci Rep* **7**, 16448, doi:10.1038/s41598-017-15434-1 (2017).

Figures

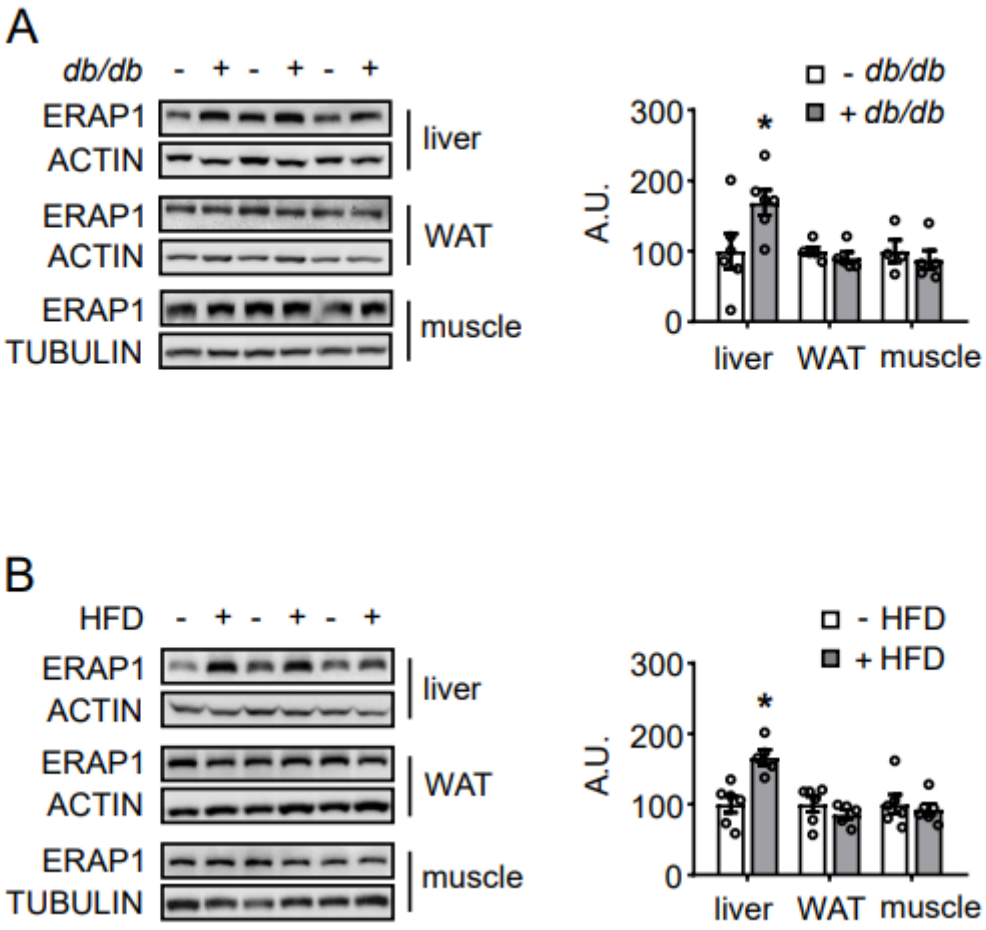

Figure 1

Elevated ERAP1 expression in the liver is related to insulin resistance. (A, B) Western blot of ERAP1 in the liver, white adipose tissue (WAT), and skeletal muscle (muscle). The right panel is the densitometric analysis of the relative abundance of ERAP1, normalized to β-actin or α-tubulin levels. Ten-week-old male wild-type (WT; −db/db) and db/db (+db/db) mice were used for (A). Four-week-old male WT mice fed a control diet (−HFD) or high-fat diet (HFD; +HFD) for 16 weeks were used for (B). All values are expressed as the mean ± SEM; n = 5 −6 mice per group, based on two independent experiments. * $P < 0.05$ for +db/db versus −db/db in (A); for +HFD versus −HFD in (B), as determined by unpaired two-tailed Student's t-test.

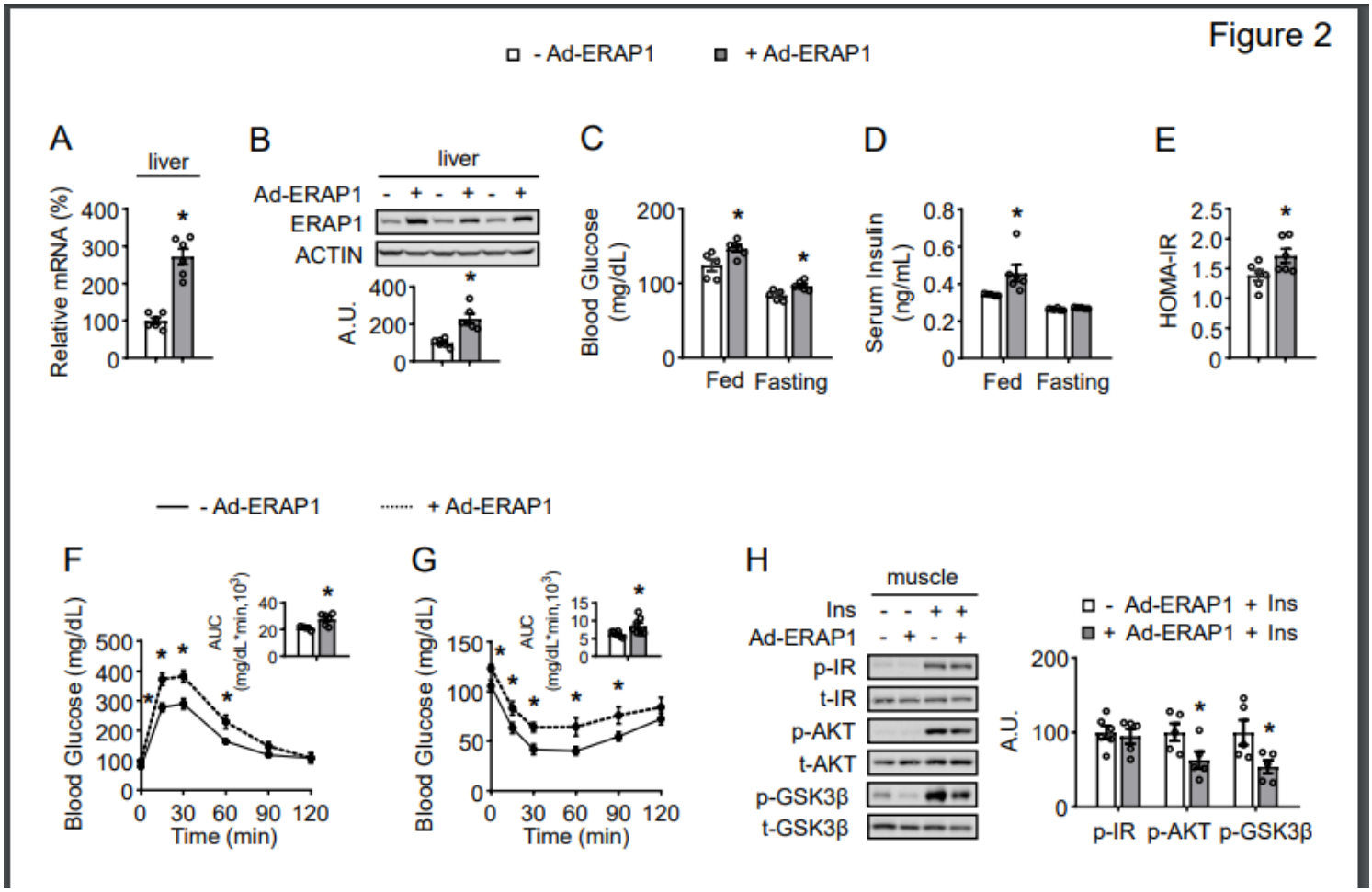

Figure 2

Overexpression of ERAP1 in the liver impairs skeletal muscle insulin sensitivity in WT mice. (A) Real-time PCR analysis of Erap1 mRNA expression in the liver. (B) Western blot of ERAP1 in the liver. The bottom panel is the densitometric analysis of the relative abundance of ERAP1 normalized to β-actin levels. (C) Fed and fasting blood glucose levels. (D) Fed and fasting serum insulin levels as determined by ELISA. (E) Calculation of the homeostatic model assessment of insulin resistance (HOMA-IR) index. (F) Glucose tolerance tests (2 g/kg). (G) Insulin tolerance tests (0.75 U/kg). (H) Western blot of phosphorylated insulin receptor on tyr1150/1151 (p-IR), protein kinase B on Ser473 (p-AKT), and glycogen synthase kinase 3β on Ser 9 (p-GSK3β) stimulated before (−Ins) or after (+Ins) 2 U/kg insulin. The right panel is the densitometric analysis of the relative abundance of phosphorylated proteins normalized to their total protein levels. Ten-week-old male wild-type (WT) mice were injected with adenovirus expressing green fluorescent protein (−Ad-ERAP1) or Ad-ERAP1 (+Ad-ERAP1) via the tail vein, and experiments were performed 6 days later. All values are expressed as the mean ± SEM; n = 5 −6 mice per group based on two independent experiments. * P < 0.05 for the effect of +Ad-ERAP1 versus −Ad-ERAP1, as determined by unpaired two-tailed Student's t-test.

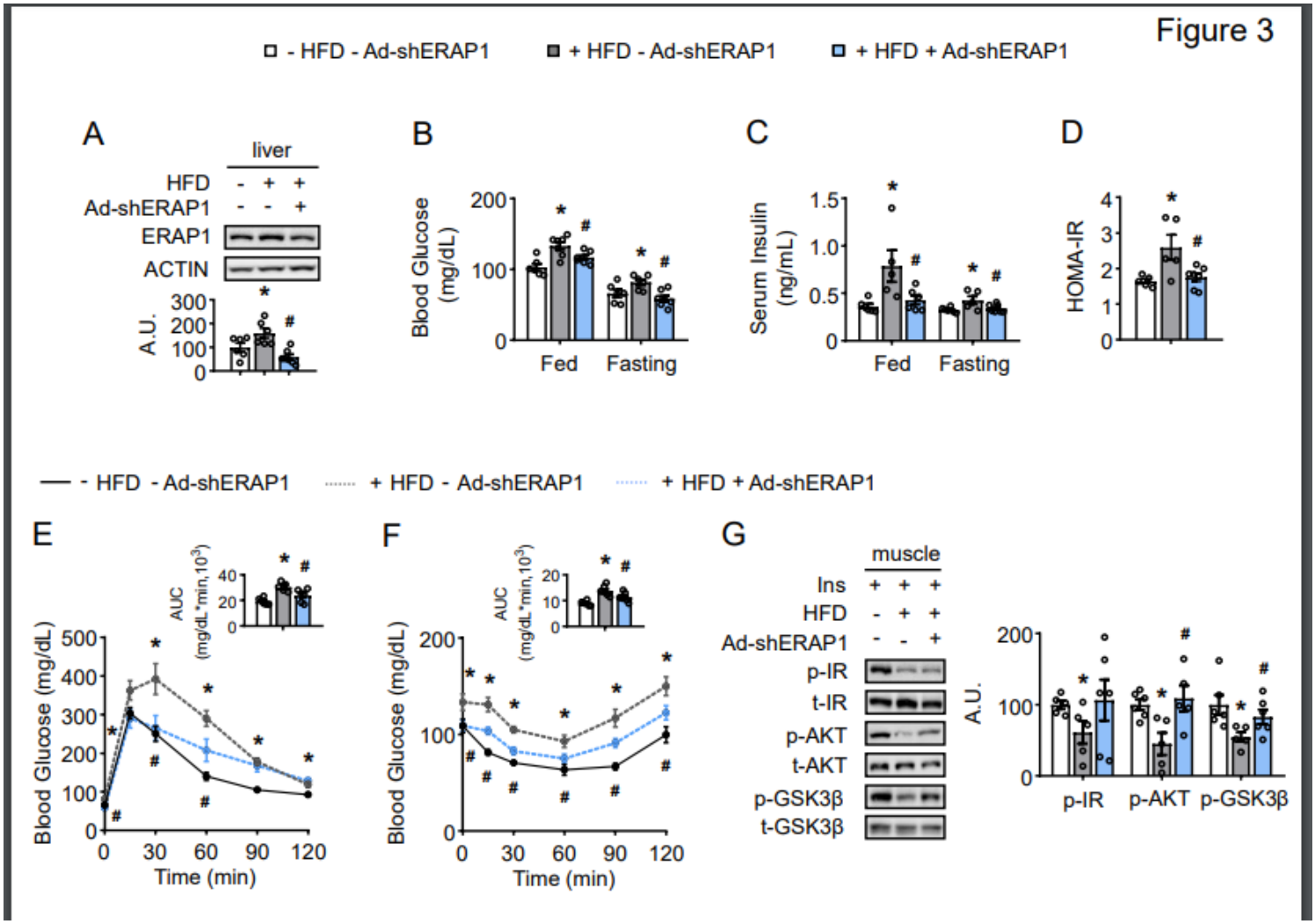

Figure 3

Liver-specific knockdown of ERAP1 ameliorates skeletal muscle insulin resistance in diabetic mice. (A) Western blot of ERAP1 in the liver. The bottom panel is the densitometric analysis of the relative abundance of ERAP1 normalized to β-actin levels. (B) Fed and fasting blood glucose levels. (C) Fed and fasting serum insulin levels as determined by ELISA. (D) Calculation of the homeostatic model assessment of insulin resistance (HOMA-IR) index. (E) Glucose tolerance tests (2 g/kg). (F) Insulin tolerance tests (0.75 U/kg). (G) Western blot of phosphorylated insulin receptor on tyr1150/1151 (p-IR), protein kinase B on Ser473 (p-AKT), and glycogen synthase kinase 3β on Ser 9 (p-GSK3β) after 2 U/kg insulin stimulation. The right panel is the densitometric analysis of the relative abundance of phosphorylated protein normalized to their total protein levels. Four-week-old male wild-type (WT) mice were fed a control diet (−HFD) or high-fat diet (HFD; +HFD) for 16 weeks and injected with negative control adenovirus (Ad-NC; −Ad-shERAP1) or Ad-shERAP1 (+Ad-shERAP1) via the tail vein, and experiments were performed 6 days later. All values are expressed as the mean ± SEM; n = 6–7 mice per group based on two independent experiments. * P < 0.05 for the effect of +HFD versus −HFD, with both groups injected with −Ad-shERAP1; # P < 0.05 for the effect of +Ad-shERAP1 versus −Ad-shERAP1, when

both groups were exposed to the +HFD condition, as determined by one-way ANONA followed by the Student-Newman-Keuls (SNK) test.

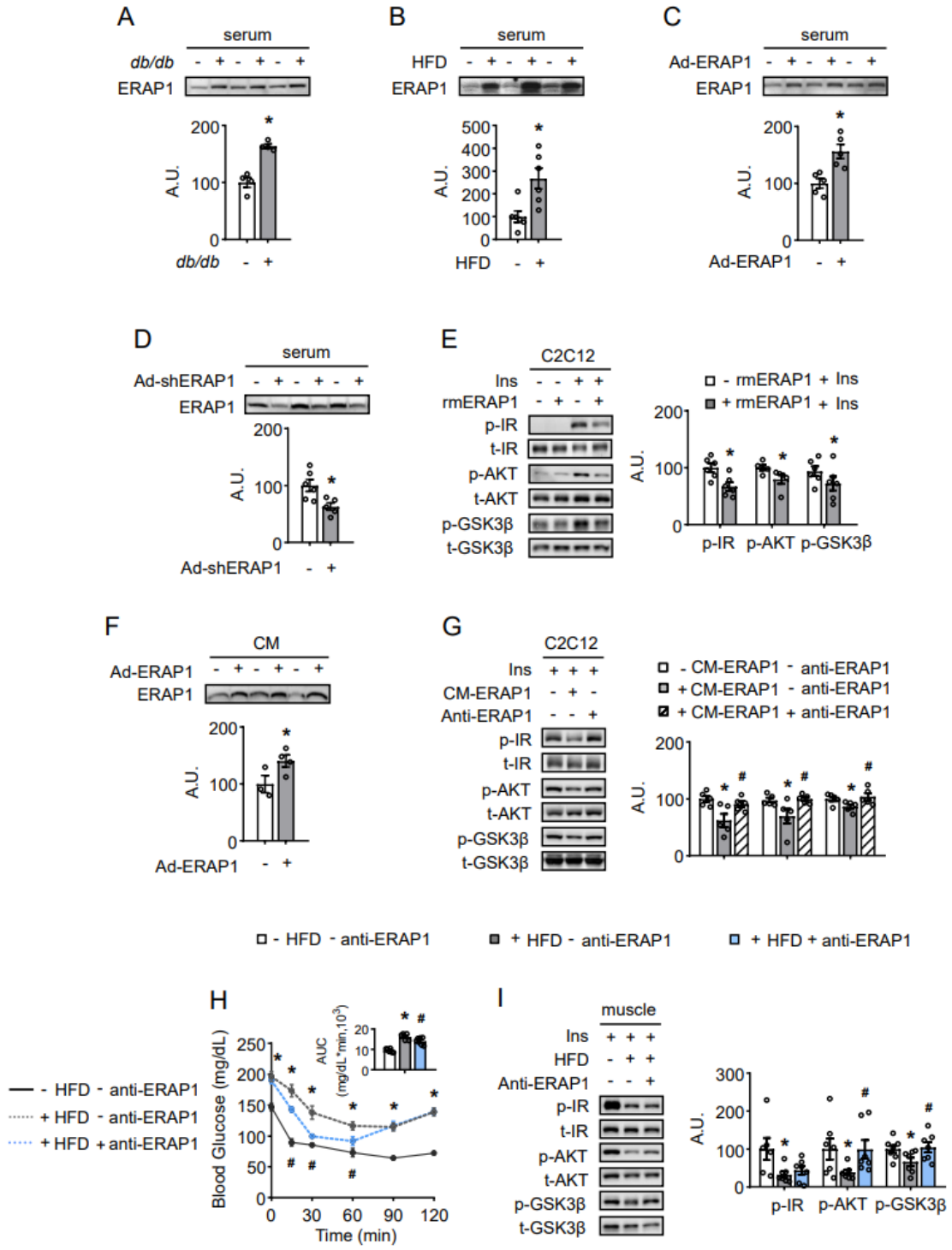

Figure 4

ERAP1 acts as a secreted factor. (A–D, F) Western blot of ERAP1. Densitometric analysis of ERAP1 relative abundance (bottom panel). (E, G and I) Western blot of phosphorylated insulin receptor on tyr1150/1151 (p-IR), protein kinase B on Ser473 (p-AKT), and glycogen synthase kinase 3β on Ser 9 (p-

GSK3β). Densitometric analysis of the relative abundance of phosphorylated protein normalized to their total protein (right panel). (H) Insulin tolerance tests (0.75 U/kg). Ten-week-old male wild-type (WT) (−db/db) or db/db (+db/db) mice were used for (A). For (B), (H), and (I), 4-week-old male WT mice were fed a control diet (−HFD) or high-fat diet (HFD; +HFD) for 16 weeks. For (C and D), 10-week-old male WT mice were injected with adenovirus expressing green fluorescent protein (Ad-GFP; −Ad-ERAP1), Ad-ERAP1 (+Ad-ERAP1), negative control adenovirus (Ad-NC; −Ad-shERAP1) or Ad-shERAP1 (+Ad-shERAP1) via the tail vein. For (E), C2C12 myotubes were incubated with (+rmERAP1) or without (−rmERAP1) 500 ng/ml recombinant mouse ERAP1 (rmERAP1) for 20 min. For (F), HepG2 cells were infected with Ad-GFP (−CM-ERAP1) or Ad-ERAP1 (+CM-ERAP1). Conditioned medium was collected 48 h later. For (G), C2C12 myotubes were incubated with conditioned medium in (F) for 48 h, and then incubated with (+anti-ERAP1) or without (−anti-ERAP1) 12 μg/ml anti-ERAP1 antibodies for the last 12 h. For (H, I), mice were intraperitoneal injected with IgG (−Anti-ERAP1) or 1 mg/kg anti-ERAP1 antibodies (+anti-ERAP1). All values are expressed as the mean ± SEM; n = 6–7 mice per group for (A–D, J, K); n = 5–6 repeats per group for (E–I); * $P < 0.05$ for +db/db versus −db/db (A), +HFD versus −HFD (B), +Ad-ERAP1 or +Ad-shERAP1 versus −Ad-ERAP1 or −Ad-shERAP1 (C and D), +rmERAP1 versus −rmERAP1 (E), +CM-ERAP1 versus −CM-ERAP1 (F, G), +CM-ERAP1 versus −CM-ERAP1 both under −anti-ERAP1 conditions (H, I), or +HFD versus −HFD both under −Anti-ERAP1 conditions (J, K); # $P < 0.05$ for the effect of +anti-ERAP1 versus −anti-ERAP1 both under +CM-ERAP1 conditions (H, I) or +anti-ERAP1 versus −anti-ERAP1 both under +HFD conditions (J, K), as determined by unpaired two-tailed Student's t-test (A–F) or by one-way ANONA followed by the Student-Newman-Keuls (SNK) test (G–I).

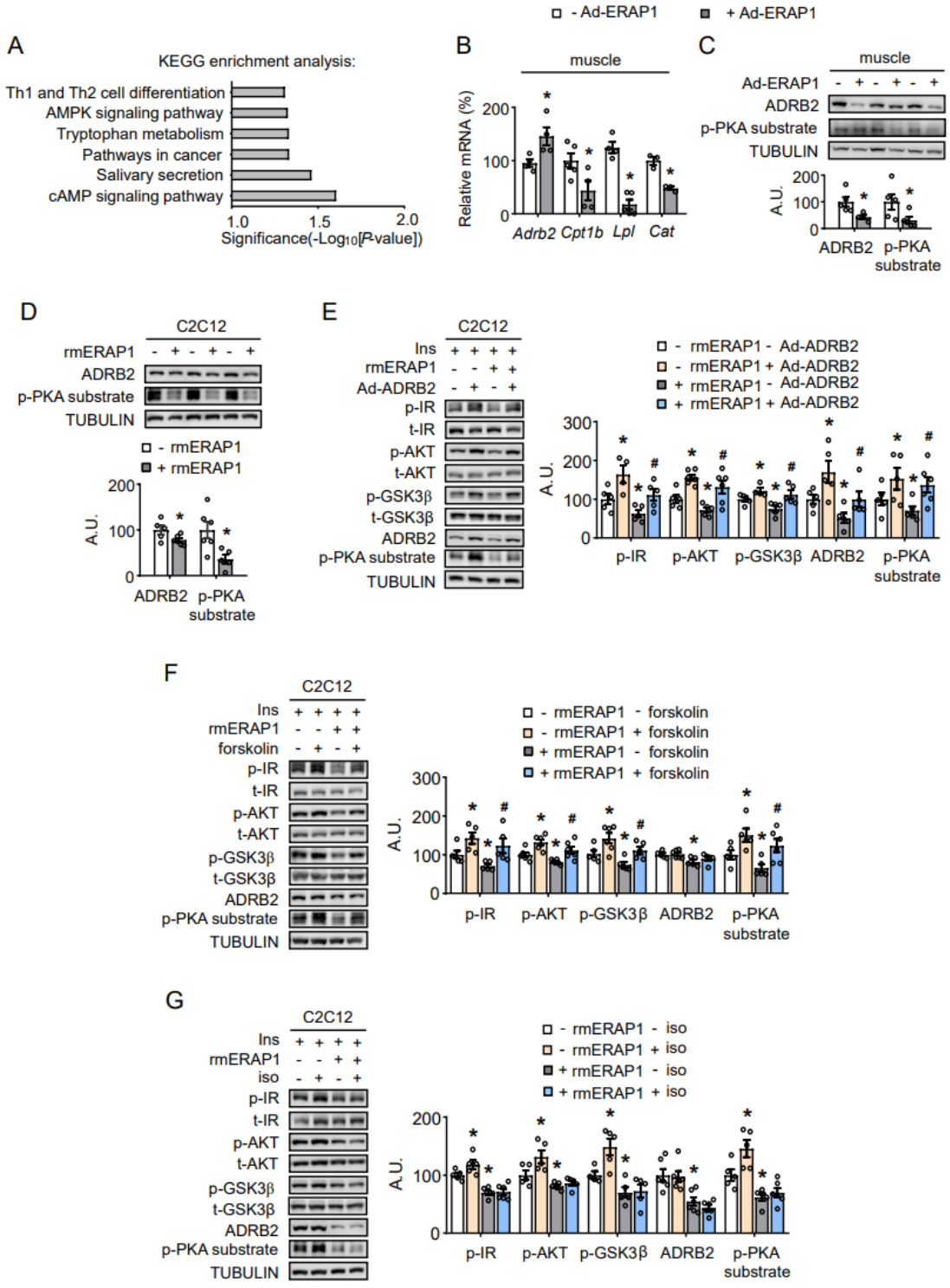

Figure 5

ERAP1 regulates skeletal muscle insulin sensitivity by decreasing ADRB2 expression. (A) KEGG enrichment analysis. (B) Real-time PCR of Adrb2, carnitine palmitoyltransferase 1B (Cpt1b), lipoprotein lipase (Lpl), and catalase (Cat) mRNA expression. (C-G) Western blot of ADRB2 and p-PKA substrate, or phosphorylated insulin receptor on tyr1150/1151 (p-IR), protein kinase B on Ser473 (p-AKT), glycogen synthase kinase 3β on Ser 9 (p-GSK3β). Densitometric analysis of the relative abundance of indicated

phosphorylated protein normalized to their total protein or α-tubulin levels (right panel). For (A–C), 10-week-old male wild-type (WT) mice were injected with adenovirus expressing green fluorescent protein (Ad-GFP; −Ad-ERAP1) or Ad-ERAP1 (+Ad-ERAP1) via the tail vein. C2C12 myotubes were incubated with (+rmERAP1) or without (−rmERAP1) 500 ng/ml recombinant mouse ERAP1 (rmERAP1) and stimulated with (+Ins) or without (−Ins) 100 nM insulin for 20 min at the same time (D). C2C12 myotubes were infected with Ad-GFP (−Ad-ADRB2) or Ad-ADBR2 (+Ad-ADRB2) for 48 h and then incubated with (+rmERAP1) or without (−rmERAP1) 500 ng/ml rmERAP1 for 2 h followed by 100 nM insulin (+Ins) stimulation for 20 min (E). C2C12 myotubes were pre-incubated with (+forskolin) or without (−forskolin) 50 μM forskolin for 24 h and then incubated with (+rmERAP1) or without (−rmERAP1) 500 ng/ml rmERAP1 for 1 h followed by 100 nM insulin (+Ins) stimulation for 20 min (F). C2C12 myotubes were incubated with (+rmERAP1) or without (−rmERAP1) 500 ng/ml rmERAP1 for 1 h and then incubated with (+iso) or without (−iso) 10 μM isoprenaline and 100 nM insulin (+Ins) for 20 min at the same time (G). All values are expressed as the mean ± SEM; n = 5–6 repeats per group. * $P < 0.05$ for the effect of +Ad-ERAP1 versus −Ad-ERAP1 (A–C), +rmERAP1 versus −rmERAP1 (D), +rmERAP1 versus −rmERAP1 under −Ad-ADRB2 conditions (E) or under −forskolin conditions (F), or under −iso conditions (G); # $P < 0.05$ for the effect of +Ad-ADRB2 versus −Ad-ADRB2 (E) or +forskolin versus −forskolin (F), or +iso versus −iso (G) under +rmERAP1 incubation, as determined by unpaired two-tailed Student's t-test (B–D) or by one-way ANONA followed by the Student-Newman-Keuls (SNK) test (E-G).

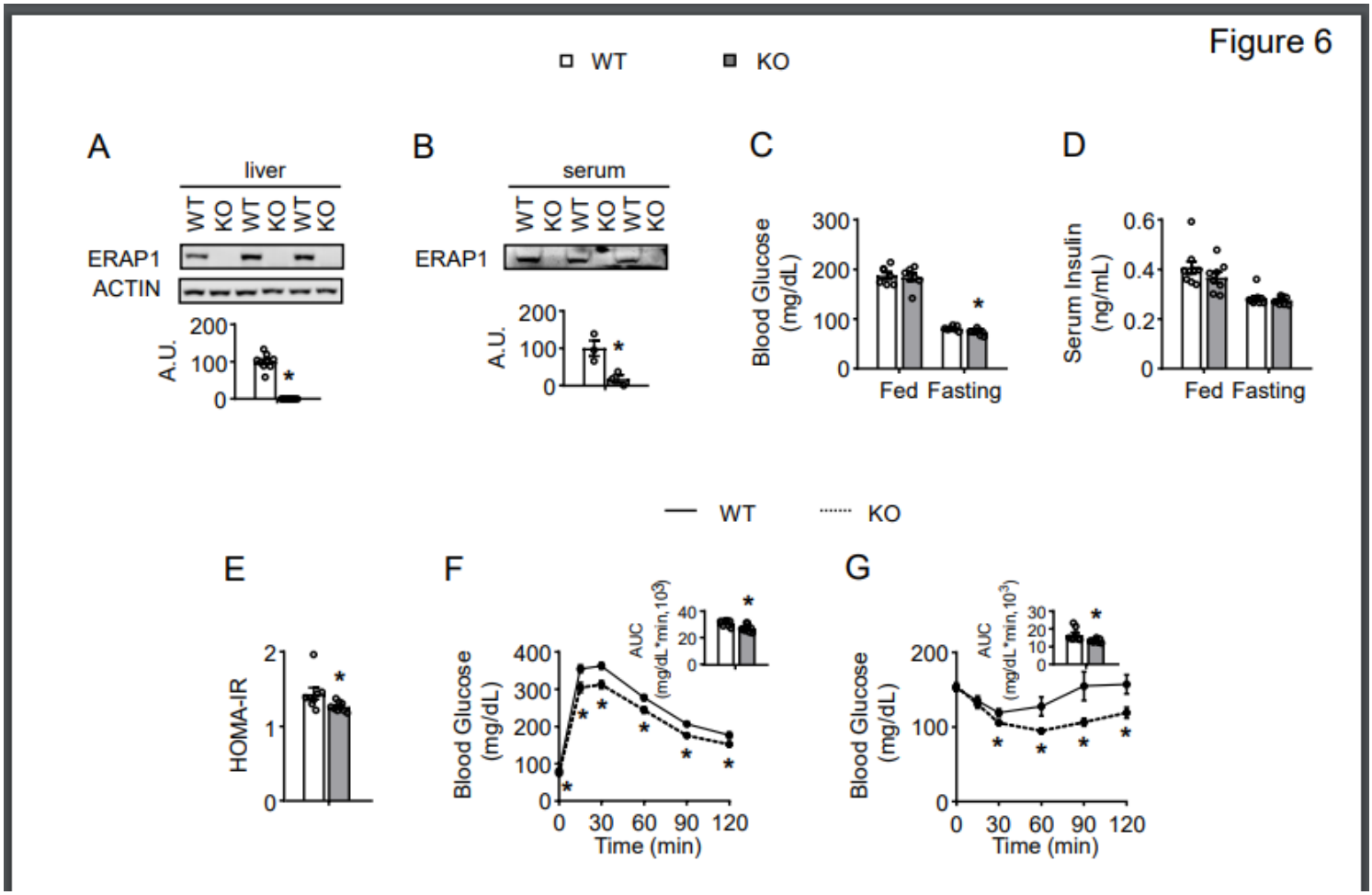

Figure 6

Global knockout of ERAP1 improves whole-body insulin sensitivity. (A) Western blot of liver ERAP1. The bottom panel is the densitometric analysis of the relative abundance of ERAP1 proteins normalized to β-actin levels. (B) Western blot of serum ERAP1. The right panel is the densitometric analysis of the relative abundance of ERAP1 protein levels. (C) Fed and fasting blood glucose levels. (D) Fed and fasting serum insulin levels as determined by ELISA. (E) Calculation of the homeostatic model assessment of insulin resistance (HOMA-IR) index. (F) Glucose tolerance tests (2 g/kg). (G) Insulin tolerance tests (0.75 U/kg). Ten-week-old wild-type (WT) and ERAP1 global knockout (KO) mice fed a control diet were used for the indicated experiments. All values are expressed as the mean ± SEM; n = 3 mice per group for (A–B); n = 7–10 mice per group for (C–G). * P < 0.05 for the difference between WT and KO mice, as determined by unpaired two-tailed Student's t-test.

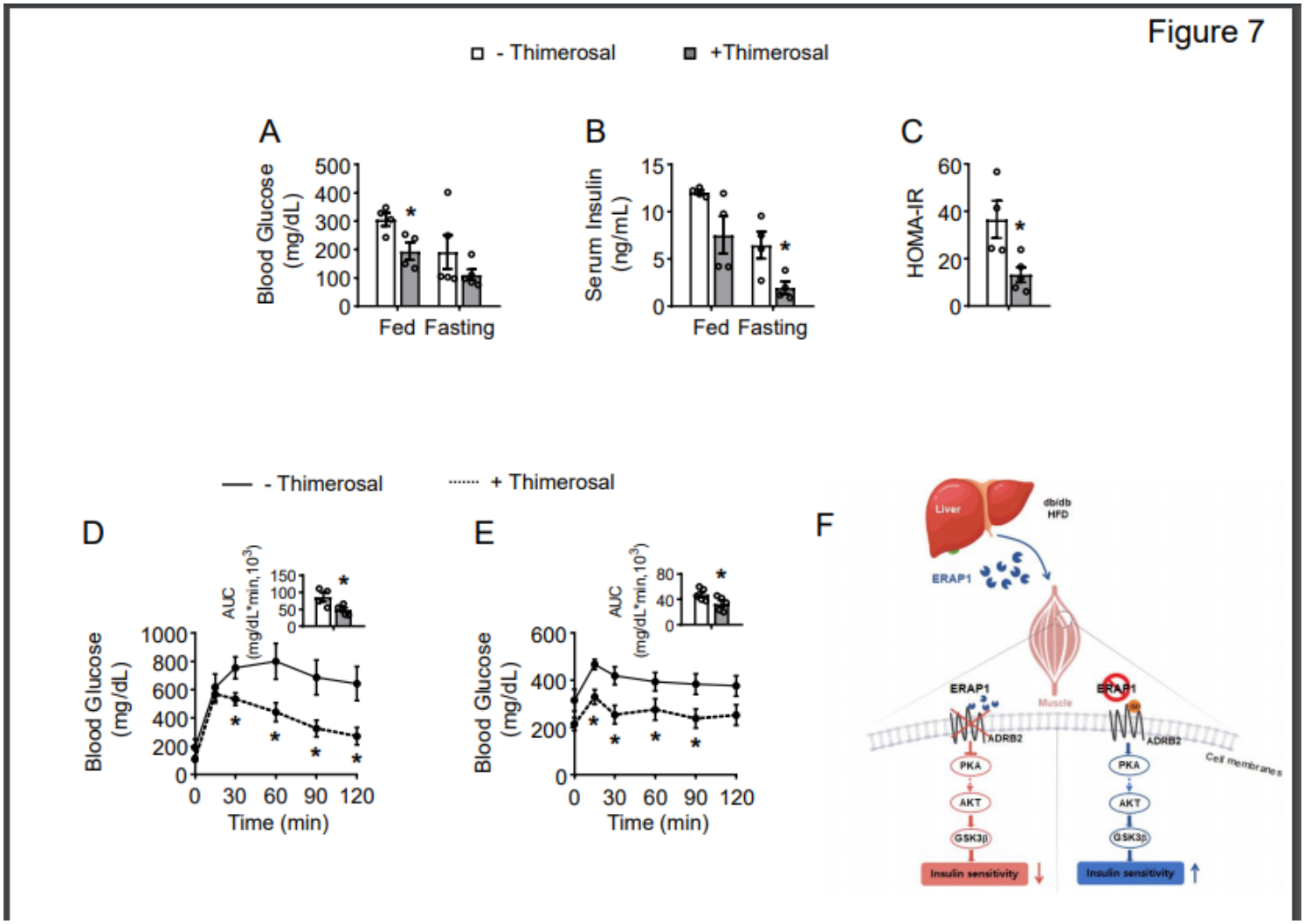

Figure 7

Inhibition of ERAP1 ameliorates insulin resistance. (A) Fed and fasting blood glucose levels. (B) Fed and fasting serum insulin levels as determined by ELISA. (C) Calculation of the homeostatic model assessment of insulin resistance (HOMA-IR) index. (D) Glucose tolerance tests (2 g/kg). (E) Insulin tolerance tests (1 U/kg). (F) Mechanistic model of the role of hepatokine ERAP1 in regulating skeletal muscle insulin sensitivity. Ten-week-old db/db mice were intraperitoneally injected with (+thimerosal) or

without (−thimerosal) 6 mg/kg thimerosal for 6 days. All values are expressed as the mean ± SEM; n = 5 −6 mice per group. * P < 0.05 for the effect of +thimerosal versus −thimerosal, as determined by unpaired two-tailed Student's t-test (A-E).

Supplementary Files

This is a list of supplementary files associated with this preprint. Click to download.

- SupplementalinformationmanuscriptNC.pdf